



## Cluster expansion and optimization of thermal conductivity in SiGe nanowires

M. K. Y. Chan,<sup>1,2</sup> J. Reed,<sup>3</sup> D. Donadio,<sup>4</sup> T. Mueller,<sup>2</sup> Y. S. Meng,<sup>2,5</sup> G. Galli,<sup>4</sup> and G. Ceder<sup>2</sup>

<sup>1</sup>*Department of Physics, Massachusetts Institute of Technology, Cambridge, MA 02139, USA*

<sup>2</sup>*Department of Materials Science and Engineering, Massachusetts Institute of Technology, Cambridge, MA 02139, USA*

<sup>3</sup>*Lawrence Livermore National Laboratory, Livermore, CA 94551, USA*

<sup>4</sup>*Department of Chemistry, University of California, Davis, Davis, CA 95616, USA*

<sup>5</sup>*Department of NanoEngineering, University of California, San Diego, La Jolla, CA 92093, USA*

(Received 29 July 2009; revised manuscript received 27 March 2010; published 7 May 2010)

We investigate the parametrization and optimization of thermal conductivity in silicon-germanium alloy nanowires by the cluster-expansion technique.  $\text{Si}_{1-x}\text{Ge}_x$  nanowires are of interest for thermoelectric applications and the reduction in lattice thermal conductivity ( $\kappa_L$ ) is desired for enhancing the thermoelectric figure of merit. We seek the minimization of  $\kappa_L$  with respect to arrangements of Si and Ge atoms in 1.5 nm diameter [111]  $\text{Si}_{1-x}\text{Ge}_x$  nanowires, by obtaining  $\kappa_L$  from equilibrium classical molecular-dynamics (MD) simulations via the Green-Kubo formalism, and parametrizing the results with a coarse-grained cluster expansion. Using genetic algorithm optimization with the coarse-grained cluster expansion, we are able to predict configurations that significantly decrease  $\kappa_L$  as verified by subsequent MD simulations. Our results indicate that superlattice-like configurations with planes of Ge show drastically lowered  $\kappa_L$ .

DOI: [10.1103/PhysRevB.81.174303](https://doi.org/10.1103/PhysRevB.81.174303)

PACS number(s): 68.65.-k, 63.20.dh, 63.22.Gh, 65.80.-g

### I. INTRODUCTION

#### A. SiGe nanowires for thermoelectric applications

Minimizing the thermal conductivity in silicon-germanium nanowires through nanostructuring is of interest for thermoelectric applications. Bulk SiGe alloys have been used for thermoelectric power generation for several decades, most notably in NASA space missions since the 1970s. The mass disorder in Si-Ge causes enhanced phonon scattering, thereby reducing the thermal conductivity without significant modification of the electronic properties. Since proposed by Hicks and Dresselhaus<sup>1,2</sup> in the 1990s, lower dimensional systems such as quantum wells,<sup>3</sup> thin films,<sup>4</sup> superlattices,<sup>5</sup> nanocomposites,<sup>6,7</sup> and nanowires<sup>8</sup> have been actively investigated for improved thermoelectric properties. Thermoelectric performance is measured by the figure of merit  $ZT = S^2 \sigma T / (\kappa_e + \kappa_L)$ , where  $S$  is the Seebeck coefficient,  $\sigma$  is the electrical conductivity,  $T$  is the temperature, and  $\kappa_e$  and  $\kappa_L$  are the electronic and lattice contributions to thermal conductivity, respectively. A key attribute of nanostructuring is the possibility for achieving high  $ZT$  by reducing  $\kappa_L$  through the confinement and enhanced scattering of phonons, without a concomitant reduction in  $\sigma$  or  $S$ . This may be possible because of the disparate wavelengths and scattering lengths of electrons vs phonons.<sup>9</sup> Experimental results show nanostructuring to be effective at reducing  $\kappa_L$ . For example, silicon nanowires with diameters from 20 to 100 nm show a thermal conductivity of 10–40 W/m K at 300 K,<sup>10</sup> compared to 124 W/m K for bulk Si.<sup>11</sup> Si/SiGe superlattice nanowires show a further fivefold reduction in thermal conductivity compared to pure Si nanowires of similar diameters.<sup>12</sup> In SiGe nanocomposites consisting of 10 nm Si nanoparticles in a Ge host,  $\kappa_L$  has been measured to be less than 2 W/m K.<sup>13</sup> Pure Si nanowires with roughened surfaces have been measured to have  $\kappa_L$  as low as 1.2 W/m K,<sup>14</sup> consistent with results of molecular-dynamics (MD) simulations for thin wires with disordered surfaces. Nanowires with rough, amorphous surfaces, and crystalline cores are particu-

larly attractive for thermoelectric applications since crystallinity is beneficial to charge mobility. The various experimental results show that  $\kappa_L$  depends sensitively not only on the size of the nanostructures but also on the type and arrangement of atoms therein. In this paper we address the question of what arrangements (i.e., configurations) of Si and Ge atoms in the crystalline core of a SiGe nanowire give the lowest possible  $\kappa_L$ , as an ultimate form of nanostructuring. In order to understand nanoscale effects on phonon spectrum, dispersion, and interactions, as well as interfacial and alloying effects, it is essential to model the dynamics at the atomic level. We also model surface roughening through the control of the size of the simulation cell. We pursue the optimization problem by expanding calculated thermal conductivities in a basis of site-occupation variables and by performing optimization with genetic algorithm.

#### B. Extending the cluster-expansion technique to thermal conductivity

Cluster expansion,<sup>15</sup> whereby properties are expanded in terms of the distribution of atoms on a topology of sites, is a powerful technique for the optimization or ensemble averaging of properties. Its most common use is in the parametrization of total energy and derivatives thereof, although there have been extensions to other properties such as band gaps<sup>16</sup> and, more recently, tensorial quantities.<sup>17</sup> The cluster expansion of total energy has been used extensively, often with *ab initio* calculations, to build effective Hamiltonians for the prediction of thermodynamic<sup>18</sup> and kinetic properties.<sup>19</sup> Unlike atomic potential models, which are rapidly evaluated but require extensive chemistry-dependent parametrization and are not universally available, or *ab initio* calculations, which are (almost) universally available but are computationally intensive, the cluster-expansion approach is a widely applicable parametrization method which allows rapid evaluations for a large number of different atomic configurations. In addition, the fitting parameters of the expansion, called effec-

tive cluster interactions (ECIs), often give important physical insights on the system.

It is desirable to investigate the applicability of the cluster-expansion approach to properties of crystalline materials not based on total energy, such as thermal conductivity. Since the evaluation of thermal conductivity is computationally intensive, even using classical molecular dynamics, the ability to parametrize the results for subsequent rapid evaluations would enable the otherwise prohibitive sampling of atomic configurations for optimization purposes. While the cluster expansion is formally exact with the inclusion of all possible clusters, in practice it is necessary to truncate the expansion to a finite number of clusters. Completely accounting for the contribution of a cluster of sites requires the determination of the ECI(s) not only for the given cluster but for all subclusters as well.<sup>20,21</sup> Therefore, truncation of the expansion generally leads to an inclusion of only short-ranged effects. In addition, it is not *a priori* clear whether thermal conductivity can be parametrized by local configurational variables alone.

The purpose of our work is hence twofold: to optimize atomic configurations in SiGe nanowires for low lattice thermal conductivity  $\kappa_L$  and to evaluate the applicability of the cluster-expansion technique for the optimization of  $\kappa_L$ . Our strategy is to determine the values of  $\kappa_L$  for a test set of atomic configurations using equilibrium MD simulations, use the cluster-expansion technique to allow rapid evaluation of  $\kappa_L$  for any configuration, and thus predict structures with the lowest  $\kappa_L$  through genetic algorithm optimization. The validity of the technique is finally checked with the direct evaluation of  $\kappa_L$  of the predicted optimal structures using MD.

## II. THERMAL CONDUCTIVITY FROM MOLECULAR DYNAMICS

### A. Computational procedures

We obtain, using equilibrium classical MD simulations, the thermal conductivity of  $\text{Si}_{1-x}\text{Ge}_x$  nanowires. The nanowires in our study are in the  $[111]$  orientation, have a circular cross section with a diameter of 1.5 nm, and have varying Ge concentration ( $0.03 < x < 0.2$ ) and Si/Ge configurations. The surfaces of the wire are not terminated by hydrogen atoms. Simulations are carried out at 300 K. An example of a simulation cell is shown in Fig. 1.

The XMD molecular-dynamics program developed by Jon Rifkin,<sup>22</sup> modified to output the heat flux for systems incorporating Si and Ge, was used to perform the MD simulations. Interactions were described by a bond order Tersoff potential<sup>23</sup> designed for C-Si-Ge systems that varies chemical bond strength according to the local coordination environment, given by

$$V_{ij} = f_c(r_{ij})[f_r(r_{ij}) + b_{ij}f_a(r_{ij})]. \quad (1)$$

Here  $f_c$  is a smooth cutoff function,  $f_r$  and  $f_a$  are repulsive and attractive pair potential terms, and the bond order term  $b_{ij}$  is a function of the number of neighboring atoms as well as bond angles and lengths. Upon initial  $NVT$  (constant particle number  $N$ , volume  $V$ , and temperature  $T$ ) equilibration,

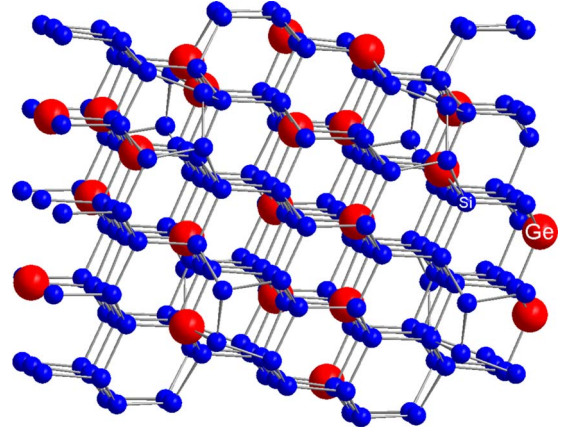


FIG. 1. (Color online) An example SiGe nanowire simulation cell (side view). Red, larger spheres denote Ge while blue, smaller spheres denote Si.

$NVE$  (constant  $N$ ,  $V$ , and total energy  $E$ ) simulations are performed with a time step of 0.8 fs. The thermal conductivity for each nanowire along the axial direction ( $z$ ) was calculated using the Kubo-Green formula

$$\kappa_{zz} = \frac{V}{k_B T^2} \lim_{t \rightarrow \infty} \int_0^t \langle J_z(t') J_z(0) \rangle dt', \quad (2)$$

where  $J$  is the heat current.

### B. Modeling the effects of surface roughness

It has been reported<sup>24</sup> that with simulation cells of length  $L \geq 10$  nm, the values of  $\kappa_L$  computed for thin, pure Si nanowires with ordered surfaces are as much as half that of bulk Si, in stark contrast to the 100 reduction in  $\kappa_L$  from bulk values for nanowires with amorphized surfaces. These computational results are consistent with experimental measurements on Si nanowires with smooth and roughened surfaces.<sup>14</sup> We are interested in investigating further reduction in the lattice thermal conductivity due to Si/Ge configurations in nanowires with roughened surfaces. However, computations with simulation cells of  $L \geq 10$  nm and wires with roughened surfaces are extremely expensive.

In the interest of computational feasibility, we mimic the effect of surface roughness by using simulation cells of 2 nm long along the axial direction. Qualitatively, the effect of using small cell sizes is the same as that of surface roughness: long-wavelength phonons cannot and do not contribute to heat transport. To verify that 2 nm (short) simulation cells may reproduce 10 nm (long) simulation cells with surface roughness, we compare the values of  $\kappa_L$  in pure Si nanowires for short, pristine vs long simulation cells with and without surface roughness. Surface roughness is produced by adding silicon atoms on the surface in two regions of 2.5 nm, at intervals of 2.5 nm. In such regions we create a disordered monolayer of Si atoms by saturating 80% of the surface dangling bonds. The system is annealed at 1600 K and then gradually quenched to room temperature, so as to stabilize the newly generated structure. The whole annealing and quenching process lasts 1.5 ns and causes no structural modi-

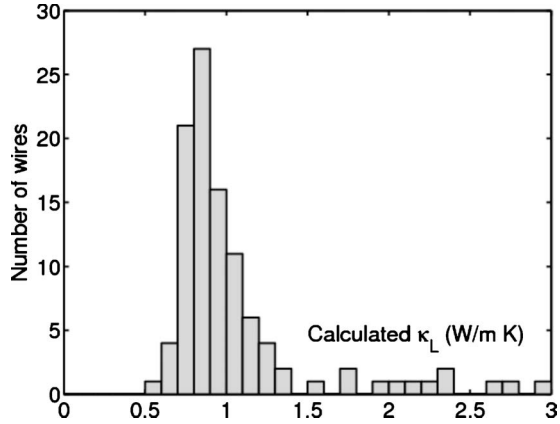


FIG. 2. Histogram of lattice thermal conductivity calculated using MD for the training set of 104 nanowires with different Si/Ge configurations.

fications either in the crystalline core of the nanowires or in the regions where the surface has not been modified. An example of the long simulation cells with surface roughness is shown in Fig. 2. We find that the value of  $\kappa_L$  for short, pristine simulation cell ( $4.1 \pm 0.3$  W/m K) is much closer to that of the long simulation cell with surface roughness ( $2.6 \pm 0.2$  W/m K) than that of the long, pristine simulation cell ( $50 \pm 7$  W/m K). Therefore, we carry out the calculation of  $\kappa_L$  for nanowires with different SiGe configurations using short, pristine simulation cells. Further verifications of the validity of this approach will be provided in Sec. V.

### C. Summary of MD results

The calculated thermal conductivities of the 104 SiGe nanowires in the training set are shown in Fig. 3. The training set configurations are selected to cover a range of compositions up to 22% Ge and provide a large variety in the distribution of Si and Ge atoms. For each configuration, the MD simulation is repeated several times and the standard deviation of the resultant  $\kappa_L$  is taken as the uncertainty. In

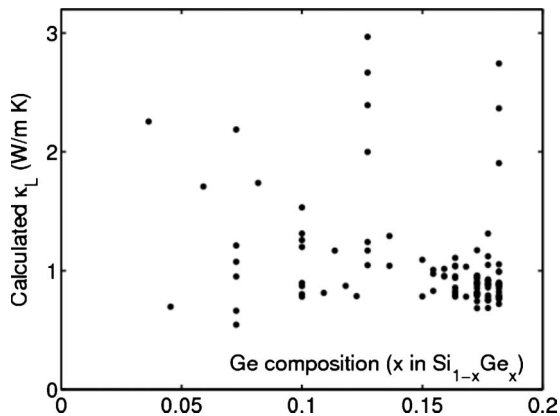


FIG. 3. Lattice thermal conductivity of nanowires with different Si/Ge configurations vs Ge composition. For SiGe nanowires in the training set, there is stronger dependence of  $\kappa_L$  on configurations within the same Ge composition range than on Ge composition.

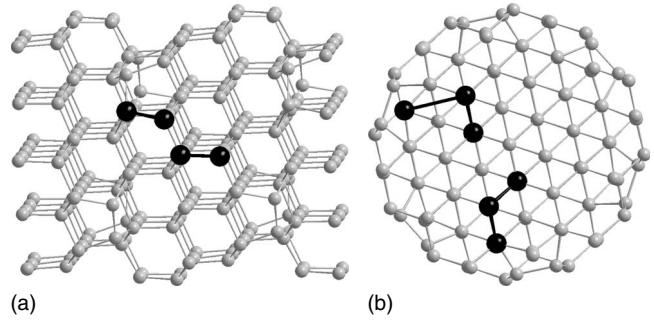


FIG. 4. Examples of clusters considered equivalent in the coarse-grained cluster expansion: (left, side view) two pair clusters that are both *surface* and *along*, and (right, end view) two triplet clusters that are both *intermediate* and *across*.

general the uncertainties are larger with larger  $\kappa_L$  and are on average about 10% of  $\kappa_L$ . The calculated values of  $\kappa_L$  range from 0.55 to 3.0 W/m K, with a mean and standard deviation of 1.1 and 0.5 W/m K, respectively. For comparison, the measured values of  $\kappa_L$  at 300 K are 9–25 W/m K for bulk  $\text{Si}_{1-x}\text{Ge}_x$  alloys ( $0.05 < x < 0.22$ ),<sup>25</sup> 15–40 W/m K for 37–115 nm diameter Si nanowire with smooth surfaces,<sup>10</sup> and 1–8 W/m K for 50–150 nm diameter Si nanowires with roughened surfaces.<sup>14</sup> Figure 4 plots the values of  $\kappa_L$  against Ge composition for each configuration and it is clear that there is no strong dependence of  $\kappa_L$  on the concentration of Ge. Therefore, the variation in  $\kappa_L$  is due predominantly to the Si/Ge configuration.

## III. THERMAL-CONDUCTIVITY CLUSTER EXPANSION

### A. Traditional cluster expansion

A traditional cluster expansion<sup>15,17</sup> for a binary alloy is an Ising-like model in which each site  $i$  in a lattice is assigned a value  $\sigma_i = \pm 1$  depending on the occupying species. Polynomials of  $\sigma_i$  of all orders form a complete orthonormal basis set in which to expand any configurational-dependent physical quantity  $Q$ , i.e.,

$$Q = \sum_{\alpha} V_{\alpha} \left( \prod_{i \in \alpha} \sigma_i \right), \quad (3)$$

where the sum is over all possible distinct clusters of sites  $\alpha$  and the coefficients of the expansion  $V_{\alpha}$  are fitting parameters known as ECIs. In practice, the ECIs are obtained by fitting Eq. (3) to the calculated values of  $Q$  (e.g., by MD simulations in the case of  $\kappa_L$ ) for a number of sample configurations. The expansion can then be used to predict values of  $Q$  for any configuration. As mentioned, a cluster expansion is necessarily truncated to clusters of reasonably small order. Symmetry is used to reduce the number of ECIs.

### B. Coarse-grained cluster expansion

For both physical and practical reasons, we perform a coarse graining of the cluster expansion. Physically, it is expected that clusters similar in location, size, and orientation would give a similar contribution to the thermal conductivity. Practically, we are limited by the number of relevant param-

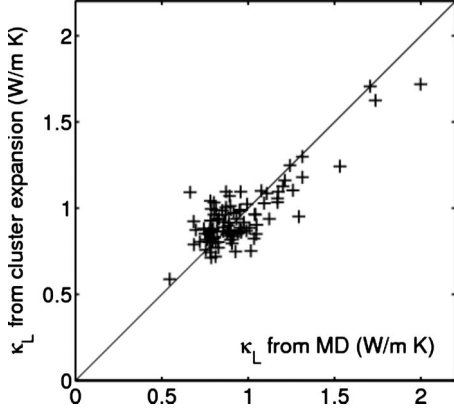


FIG. 5. After performing the fitting procedures, the values of  $\kappa_L$  predicted from coarse-grained cluster expansion [Eq. (5)] vs those calculated from MD.

eters that can be extracted. The low symmetry in a nanowire leads to a large number of symmetrically inequivalent clusters and therefore a large number of ECIs ( $V_\alpha$ 's). Together with the inherent noise in the values of  $\kappa_L$  due to the stochastic nature of MD simulations, such a large number of parameters leads to over-fitting and diminished predictive power of the cluster expansion. Recently, approaches have been developed to deal with such low-symmetry situations by imposing nonuniform prior probability densities on the ECIs.<sup>26</sup> We will, however, use a coarse-graining approach as described below.

### 1. Coarse-graining procedures

Coarse-graining procedures are performed to group physically similar, but symmetrically inequivalent, clusters (points, pairs, and triplets) in the nanowire. All clusters in a group are considered equivalent in the coarse-grained cluster expansion and their ECIs have the same value. Equivalent clusters have (a) similar distance from the axis of the nanowire and, for pairs and triplets only, (b) similar extents along the length of the nanowire. For classification (a), clusters entirely within the inner 10% of the cross-sectional area of the nanowire are considered *core*, those entirely outside the inner 90% are considered *surface*, and the rest are considered *intermediate*. For (b), clusters contained in planes parallel/nearly parallel to nanowire cross sections are considered *across* while those in planes parallel/nearly parallel to the nanowire axis are considered *along*, and all others are *oblique*. The coarse-graining procedure gives, for the simulation nanowires described in Sec. II, 40 coarse-grained point, pair, and triplet clusters, with a maximum spatial extent of 4.5 Å. Figure 5 shows examples of clusters that are considered equivalent in the coarse-graining procedure.

### 2. Fitting procedures

The ECIs in the coarse-grained cluster expansion are obtained by the following procedures: we expand the values of  $\kappa_L$  for the  $N$  wires in the training set as

$$\kappa_{Ln} = \sum_{\beta} V_{\beta} \left\langle \prod_{i \in \alpha} \sigma_{in} \right\rangle_{\beta} \equiv \sum_{\beta} V_{\beta} \Phi_{\beta n}, \quad (4)$$

where  $n=1, \dots, N$ ,  $\beta$  labels a coarse-grained cluster, and  $\langle \cdot \rangle_{\beta}$  refers to average over all clusters  $\alpha$  coarse grained into  $\beta$ .

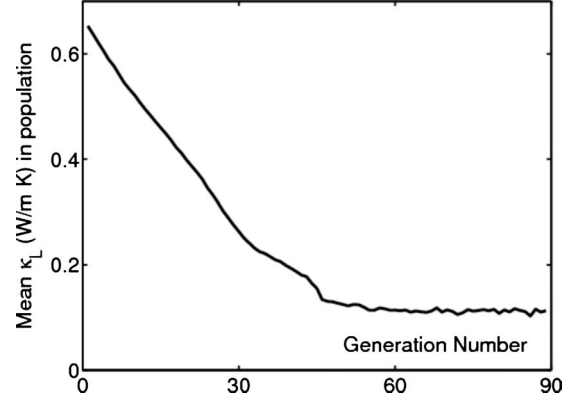


FIG. 6. Convergence of  $\kappa_L$  with generation number in genetic algorithm optimization.

The  $\Phi_{\beta n}$ 's are then orthonormalized, i.e., Eq. (4) is transformed into

$$\kappa_{Ln} = \sum_{\beta'} \tilde{V}_{\beta'} \tilde{\Phi}_{\beta' n}, \quad (5)$$

where  $\sum_{\beta'} \tilde{\Phi}_{\beta' m} \tilde{\Phi}_{\beta' n} = \delta_{mn}$ . Note that each  $\beta'$  now represents a linear combination of coarse-grained clusters. The values of the transformed ECIs  $\tilde{V}_{\beta'}$  are obtained from least square fitting of Eq. (5). Unlike the ECIs in the cluster expansion of total energy, which are expected to fall off as a function of distance, there is no *a priori* known behavior for the values of  $\tilde{V}_{\beta'}$ . In order to screen out irrelevant parameters, the least-square fit is repeated  $N$  times leaving one configuration out each time. For each  $\beta'$ , the value of  $\tilde{V}_{\beta'}$  varies with each leave-one-out fit, with a mean  $\bar{V}_{\beta'}$  and standard deviation  $\sigma_{\beta'}$ . A linear combination of clusters  $\beta'$  is considered irrelevant and removed if  $|\bar{V}_{\beta'}| < \sigma_{\beta'}$ . Roughly a quarter of the 40 ECIs (corresponding to the 40 coarse-grained clusters described above) are removed by this approach. The fit is then redone with the remaining set of  $\beta'$  and the resultant  $\tilde{V}_{\beta'}$  transformed to obtain the original ECIs  $V_{\beta}$ .

### 3. Meta cluster expansion

Because of the noise inherent in the MD values of  $\kappa_L$ , it is difficult to ascertain the accuracy of any set of ECIs from a single fit. Figure 6 shows an example of the values of  $\kappa_L$  predicted from coarse-grained cluster expansion [Eq. (5)] vs those calculated from MD. In this fit, the root-mean-squared error is 0.13 W/m K and the cross-validation score is 0.16 W/m K. In light of such uncertainties, we record multiple sets of ECIs obtained from different leave-one-out fits and different fitting procedures (e.g., different thresholds for choosing relevant linear combination of clusters  $\beta'$ , or different subset of data by range of calculated  $\kappa_L$  values or Ge concentration). Instead of a single cluster expansion we obtained a group of expansions—a *meta cluster expansion*—with different sets of ECIs  $\{V_{\beta}\}$ , all of which are consistent with the given MD results, as measured by the root-mean-squared and cross-validation errors. For any configuration, there is a range of predicted values of  $\kappa_L$  from the different

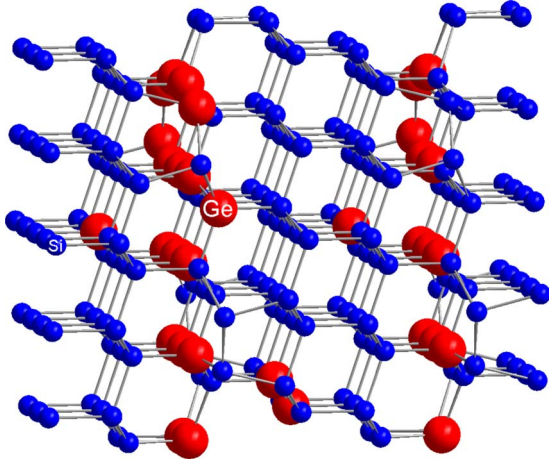


FIG. 7. (Color online) An example of a configuration found by cluster expansion and genetic algorithm optimization and verified by MD to have low  $\kappa_L$  (side view).

sets of ECIs in the meta cluster expansion, which are used together in the optimization procedure described below.

#### IV. THERMAL-CONDUCTIVITY PREDICTION AND OPTIMIZATION

##### A. Optimization by genetic algorithm

We use the thermal conductivity meta cluster expansion together with a genetic algorithm to evolve a trial population into configurations with optimal (lowest)  $\kappa_L$ . As in standard genetic algorithm implementations, pairs of nanowires with different Si/Ge configurations are mated by joining lateral or cross-sectional halves of each parent and mutations are stochastically introduced to the resultant offspring. The fitness of each configuration, i.e.,  $\kappa_L$  where a lower value is considered more fit, is evaluated by the meta cluster expansion obtained in Sec. III. We require that the predicted values are robust, i.e., the different sets of ECIs in the meta cluster expansion predict consistent values of  $\kappa_L$ , or else we consider the prediction unreliable and the configuration is discarded. To determine the consistency of predicted values of  $\kappa_L$ , we calculate the uncertainty in the predicted values based on the uncertainties in  $V_\beta$ , which are in turn derived from  $\sigma_\beta$ . If the difference in two predicted values is larger than the uncertainties added in quadrature, the predictions are not consistent. At each generation, the fittest configurations are kept and a random sample of the remainder added in to ensure genetic diversity. Any exact duplicates are removed and the genetic algorithm optimization is carried out until convergence of the mean value of  $\kappa_L$  among the wires in the population is reached, which generally occurs within 100 generations. An example of the evolution of the mean value of  $\kappa_L$  with generation number is shown in Fig. 7.

It is important to note that while the meta cluster expansion approach is able to predict low- $\kappa_L$  structures, the predicted values of  $\kappa_L$  for these structures are often unphysical, i.e., very close to zero or negative. The error in predicted values of  $\kappa_L$  can be traced back to errors in the ECIs, which in turn originate from the noise inherent in values of  $\kappa_L$

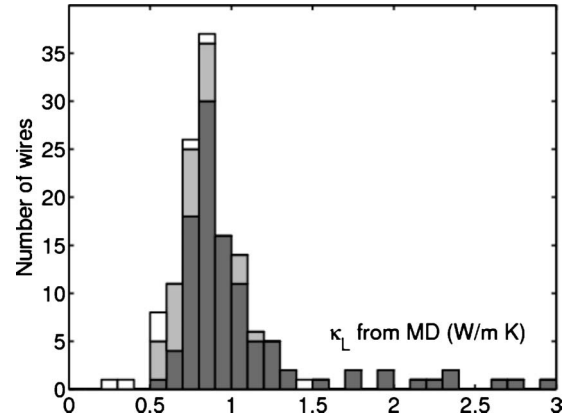


FIG. 8. Histogram of  $\kappa_L$  calculated with MD for (a) the original training data (dark gray), (b) predicted low- $\kappa_L$  configurations from cluster expansion and genetic algorithm optimization (light gray), and (c) configurations with perfect planes of Ge (white).

calculated from MD. Nonetheless, we use the meta cluster expansion and genetic algorithm optimization as a tool in finding optimal configurations rather than to predict precise values of  $\kappa_L$ . To check the effectiveness of this approach, we use MD to obtain values of  $\kappa_L$  for a selected sample of predicted low- $\kappa_L$  configurations.

##### B. Predicted low- $\kappa_L$ configurations

Figure 8 shows an example of a configuration predicted to have low  $\kappa_L$  at the end of genetic algorithm optimization. While one might expect disordered configurations to have lower  $\kappa_L$ , the meta cluster expansion and optimization algorithm predicts otherwise. Many predicted low- $\kappa_L$  configurations consist predominantly of Ge clusters of the *across* type, i.e., have almost complete planes of Ge perpendicular to the direction of the wire, instead of a randomized distribution. Such configurations are reminiscent of the Si/SiGe superlattice structures previously proposed,<sup>5</sup> albeit ones with single-atomic layers of Ge rather than segments.

To check the validity of the cluster expansion, the predicted low  $\kappa_L$  configurations, as well as those with perfect planes of Ge, are investigated using MD simulations. Figure 9 shows the  $\kappa_L$  values of these configurations obtained from MD as compared to those of the training set. Out of 28 configurations predicted to have low  $\kappa_L$  by the meta cluster expansion and genetic algorithm optimization, *one* has  $\kappa_L$  lower than all configurations in the training set, 16 (57%) have  $\kappa_L$  at or below the tenth percentile among the training set, and 24 (86%) are at or below the 50th percentile. Therefore, we can see that although the meta cluster expansion did not yield a particular configuration with drastically lower  $\kappa_L$ , it is effective in constructing a population of low- $\kappa_L$  configurations; this means that the expansion captures some physical factors governing configurational dependence of thermal conductivity. More remarkably, one of the superlattice-like configurations with complete planes of Ge (see Fig. 10), derived from idealizing the predicted configuration shown in Fig. 8, is found to have  $\kappa_L = 0.23 \pm 0.05$  W/m K, compared to a minimum of 0.55 W/m K and a mean of 1.1 W/m K for

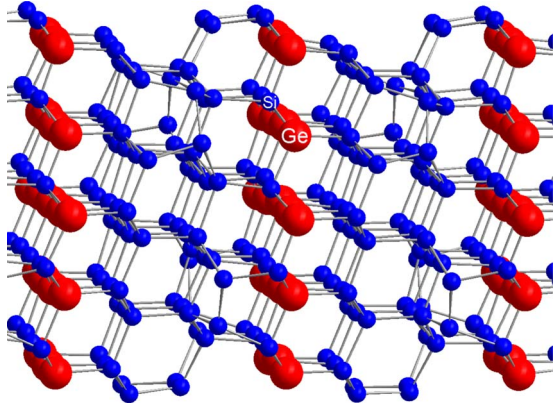


FIG. 9. (Color online) Superlatticelike configuration with the lowest value of  $\kappa_L$  as computed by MD (side view).

the training set. The reason why this specific superlatticelike configuration with very low  $\kappa_L$  was not obtained from the genetic algorithm optimization may stem from noise in the ECIs or limitations of the optimization procedures. The fact that the superlatticelike configuration is so similar to a configuration predicted to have low  $\kappa_L$  confirms that cluster expansion is a viable approach for the search of structures with optimal thermal conductivity.

**V. SHORT-RANGE ORDERING FOR REDUCING  $\kappa_L$**

In this section we offer heuristic arguments for the mechanisms by which  $\kappa_L$  is reduced and by which the coarse-grained cluster expansion is able to predict low- $\kappa_L$  configurations. We note the similarity of the values of  $\kappa_L$  in two cases: the ones computed with MD (mean=1.1 W/m K) and those measured in 52-nm-diameter Si nanowires with surface roughness on the scale of several nanometers ( $1.2 \pm 0.1$  W/m K).<sup>14</sup> In both cases, the  $\kappa_L$  values are near or below the bulk amorphous minimum thermal conductivity limit,<sup>27</sup> similar to what have been observed in other nanocrystalline systems,<sup>28</sup> despite unambiguous crystallinity. In both cases, the values of  $\kappa_L$  are an order of magnitude lower than in similar wires with longer-range order [longer simulation cells in MD (Refs. 24 and 29) or smooth-surfaced nanowires in measurements<sup>14</sup>].

**A. Removing long-range order lowers  $\kappa_L$**

In the case of our MD simulations, using 2-nm-long simulation cells excludes thermal transport by longer wavelength phonons; introducing longer-wavelength phonons by increas-

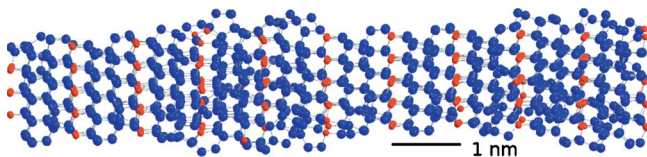


FIG. 10. (Color online) A 10-nm-long simulation cell with surface roughness at 2.5 nm intervals (side view). The SiGe alloy configuration is superlatticelike as in Fig. 9.

TABLE I. Comparison of  $\kappa_L$ (W/m K) as obtained by MD for nanowires with different SiGe configurations using short (2 nm) simulation cells and long (10 nm) simulation cells with and without surface roughness.

Configuration	$\kappa_L$ (W/m K)		
	Length surface		
	Short pristine	Long pristine	Long roughened
Pure Si	$4.1 \pm 0.3$	$50 \pm 7$	$2.6 \pm 0.2$
As in Fig. 8 <sup>a</sup>	$0.53 \pm 0.1$	$39 \pm 8$	$1.5 \pm 0.2$
As in Fig. 10 <sup>b</sup>	$0.23 \pm 0.05$	$48 \pm 10$	$1.0 \pm 0.1$

<sup>a</sup>A structure found by cluster expansion and genetic algorithm optimization to have a low  $\kappa_L$ .

<sup>b</sup>An idealization of the above, with complete planes of Ge.

ing the simulation cells length to, e.g., 12 nm increases  $\kappa_L$  by an order of magnitude. In a qualitatively similar fashion, in wires with rough surfaces,<sup>14</sup> heat-carrying long-wavelength phonons are strongly suppressed by surface scattering and their contribution to  $\kappa_L$  is greatly reduced, thus dramatically lowering the thermal conductivity compared to long, pristine wires without surface disorder.

To verify that the suppression of long-range order is the key reason for the values of  $\kappa_L$  we obtained for the SiGe alloy nanowires and that the use of 2-nm-long (short) simulation cells adequately capture the consequences of such a suppression, we compute  $\kappa_L$  by the Kubo-Green approach for 10-nm-long (long) simulation cells with and without surface roughness at  $\sim 2.5$  nm intervals. The procedures for introducing surface roughness are as described in Sec. II B. We perform the simulations on SiGe alloy nanowires corresponding to the lowest thermal conductivities in the short simulation cells (e.g., as shown in Figs. 8 and 10). The results are summarized in Table I. We find, as previously reported,<sup>24</sup> and as in the case of pure Si nanowires described in Sec. II B, that long cells with pristine surfaces have bulk-like thermal conductivity. We find also that long cells with surface roughness retain the same range of  $\kappa_L$  as short cells with pristine surfaces. The results are consistent with the postulate that removal of long-range order by using short simulation cells captures most of the effects of a roughened surface.

**B. Cluster expansion allow for further optimization of  $\kappa_L$**

Given that low values of  $\kappa_L$  near the amorphous limits are likely achieved with the exclusion of long-wavelength phonons, it is reasonable that a coarse-grained cluster-expansion approach which includes only local ordering would be able to treat the effects of further variations in  $\kappa_L$  arising from atomic configurations. In fact, from Table I, we find that  $\kappa_L$  has little or no configurational dependence for long cells with pristine surfaces (the three values in column 2 are not significantly different) but has similar configurational dependence for long cells with roughened surfaces as for short cells (columns 1 and 3 correlate). This result strongly

suggests that the local cluster-expansion approach is applicable for systems with reduced long-range order and that the physical effects of surface roughness can be adequately approximated by the exclusion of long-wavelength phonons using short simulation cells.

The precise mechanism for the configurational dependence of  $\kappa_L$  in SiGe nanowires with reduced long-range order is not known. Fourier analysis of the heat flux and explicit computation of the phonon modes and dispersion reveals persistent nonpropagating (zero-velocity) modes at 1–4 THz. Further analysis of the contributions of coherent, phononlike vs incoherent, diffusive heat transport, as well as phonon lifetimes and phonon-phonon interactions are needed. Such analysis may also shed light on the reasons for the low values of  $\kappa_L$  for structures with complete planes of Ge.

## VI. CONCLUSION

We demonstrate in this paper the feasibility of using the cluster-expansion technique to parametrize and optimize thermal conductivity. Compared to the total energy  $E$ , the computation of lattice thermal conductivity  $\kappa_L$  is much more expensive; therefore an efficient parametrization is highly

desirable. Yet the computation of  $\kappa_L$  is also fraught with more uncertainties than that of  $E$ , which makes such a parametrization difficult. We find that instead of using a traditional cluster expansion, in which each symmetrically inequivalent cluster enters, a coarse-grained approach is effective; instead of using a single set of cluster-expansion parameters, a meta cluster-expansion approach can be adopted to take into account variations due to noise in the data as well as choice of fitting parameters. Using these approaches, we are able to discover populations with generally lower  $\kappa_L$  as well as configurations similar to those which drastically lower thermal conductivity. We find that configurations with complete planes of Ge atoms have the lowest  $\kappa_L$  compared to other configurations. We find strong evidence that the low  $\kappa_L$  values obtained, close to the bulk amorphous limit, are due to the absence of long-range order in the simulations and that such absence allows a local cluster-expansion approach to optimize  $\kappa_L$  in this low- $\kappa_L$  regime.

## ACKNOWLEDGMENTS

The authors acknowledge funding from DARPA-PROM program under Grant No. W911NF-06-1-0175. In addition, D. Donadio and G. Galli acknowledge funding from DOE SciDAC under Grant No. DEFC02-06ER25794.

- 
- <sup>1</sup>L. D. Hicks and M. S. Dresselhaus, *Phys. Rev. B* **47**, 12727 (1993).
- <sup>2</sup>L. D. Hicks and M. S. Dresselhaus, *Phys. Rev. B* **47**, 16631 (1993).
- <sup>3</sup>L. D. Hicks, T. C. Harman, X. Sun, and M. S. Dresselhaus, *Phys. Rev. B* **53**, R10493 (1996).
- <sup>4</sup>R. Venkatasubramanian, E. Siivola, T. Colpitts, and B. O'Quinn, *Nature (London)* **413**, 597 (2001).
- <sup>5</sup>Y. Wu, R. Fan, and P. Yang, *Nano Lett.* **2**, 83 (2002).
- <sup>6</sup>J. P. Heremans, C. M. Thrush, D. T. Morelli, and M.-C. Wu, *Phys. Rev. Lett.* **88**, 216801 (2002).
- <sup>7</sup>B. Poudel, Q. Hao, Y. Ma, Y. Lan, A. Minnich, B. Yu, X. Yan, D. Wang, A. Muto, D. Vashaee, X. Chen, J. Liu, M. S. Dresselhaus, G. Chen, and Z. Ren, *Science* **320**, 634 (2008).
- <sup>8</sup>A. Abramson, W. C. Kim, S. Huxtable, H. Yan, Y. Wu, A. Majumdar, C.-L. Tien, and P. Yang, *J. Microelectromech. Syst.* **13**, 505 (2004).
- <sup>9</sup>D. Cahill, K. Goodson, and A. Majumdar, *ASME J. Heat Transfer* **124**, 223 (2002).
- <sup>10</sup>D. Li, Y. Wu, P. Kim, L. Shi, P. Yang, and A. Majumdar, *Appl. Phys. Lett.* **83**, 2934 (2003).
- <sup>11</sup>*CRC Handbook of Chemistry and Physics*, 88th ed., edited by D. R. Lide (CRC Press/Taylor & Francis, Boca Raton, FL, 2007).
- <sup>12</sup>D. Li, Y. Wu, R. Fan, P. Yang, and A. Majumdar, *Appl. Phys. Lett.* **83**, 3186 (2003).
- <sup>13</sup>M. S. Dresselhaus, G. Chen, M. Y. Tang, R. G. Yang, H. Lee, D. Z. Wang, Z. F. Ren, J. P. Fleurial, and P. Gogna, in *Materials and Technologies for Direct Thermal-to-Electric Energy Conversion*, MRS Symposia Proceedings No. 886 (Materials Research Society, Warrendale, PA, 2005).
- <sup>14</sup>A. I. Hochbaum, R. Chen, R. D. Delgado, W. Liang, E. C. Garnett, M. Najarian, A. Majumdar, and P. Yang, *Nature (London)* **451**, 163 (2008).
- <sup>15</sup>J. M. Sanchez, F. Ducastelle, and D. Gratias, *Physica A* **128**, 334 (1984).
- <sup>16</sup>A. Franceschetti and A. Zunger, *Nature (London)* **402**, 60 (1999).
- <sup>17</sup>A. van de Walle, *Nature Mater.* **7**, 455 (2008).
- <sup>18</sup>F. Zhou, T. Maxisch, and G. Ceder, *Phys. Rev. Lett.* **97**, 155704 (2006).
- <sup>19</sup>A. Van der Ven, G. Ceder, M. Asta, and P. D. Tepesch, *Phys. Rev. B* **64**, 184307 (2001).
- <sup>20</sup>M. H. F. Sluiter and Y. Kawazoe, *Phys. Rev. B* **71**, 212201 (2005).
- <sup>21</sup>N. A. Zarkevich and D. D. Johnson, *Phys. Rev. Lett.* **92**, 255702 (2004).
- <sup>22</sup><http://xmd.sourceforge.net/about.html>
- <sup>23</sup>J. Tersoff, *Phys. Rev. B* **37**, 6991 (1988).
- <sup>24</sup>D. Donadio and G. Galli, *Phys. Rev. Lett.* **102**, 195901 (2009).
- <sup>25</sup>B. Abeles, *Phys. Rev.* **131**, 1906 (1963), and references therein.
- <sup>26</sup>T. Mueller and G. Ceder, *Phys. Rev. B* **80**, 024103 (2009).
- <sup>27</sup>G. A. Slack, in *Solid State Physics*, edited by F. S. H. Ehrenreich and D. Turnbull (Academic Press, New York, 1979), Vol. 34, p. 1.
- <sup>28</sup>C. Chiritescu, D. G. Cahill, N. Nguyen, D. Johnson, A. Bodapati, P. Keblinski, and P. Zschack, *Science* **315**, 351 (2007).
- <sup>29</sup>D. Donadio and G. Galli, *Phys. Rev. Lett.* **99**, 255502 (2007).